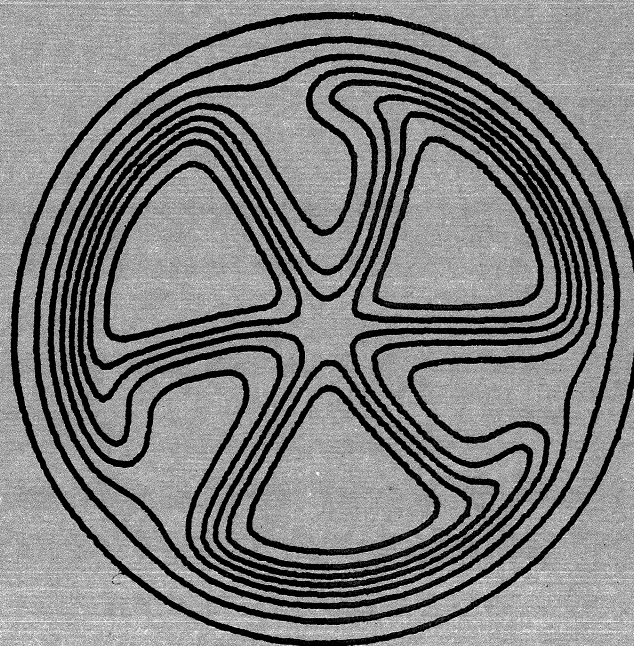


MICHIGAN STATE UNIVERSITY

CYCLOTRON LABORATORY

STUDY OF THE STRUCTURE OF ^{62}Zn and ^{64}Zn
THROUGH (p,t) REACTIONS AT 35 MeV

R.A. HINRICHS and D.M. PATTERSON



Study of the Structure of ^{62}Zn and ^{64}Zn
Through (p,t) Reactions at 35 MeV*

R. A. Hinrichs

Department of Physics, State University of New York,
College at Oswego, Oswego, N. Y. 13126

and

Cyclotron Laboratory, Michigan State University,
E. Lansing, Michigan 48823

and

D. M. Patterson

Cyclotron Laboratory, Michigan State University,
E. Lansing, Michigan 48823

ABSTRACT

Energy levels in ^{62}Zn and ^{64}Zn have been investigated via the (p,t) reaction at 35 MeV. Many new levels are reported up to an excitation energy of 5.3 MeV, with spin and parity assignments determined for most levels, including the 0^+ member of the two phonon triplet at 2.33 MeV. A comparison between the states populated in these two reactions is made. Standard distorted-wave calculations give reasonable agreement with the data. However, 3^- and 4^+ states cannot be unambiguously distinguished.

[NUCLEAR REACTIONS ^{64}Zn (p,t) ^{62}Zn , $E = 35$ MeV,
 ^{62}Zn (p,t) ^{64}Zn , $E = 35$ MeV; measured $\sigma(E, \theta)$;
 ^{62}Zn , ^{64}Zn deduced levels, J, π .

*Work supported in part by the National Science Foundation.

I. INTRODUCTION

The nucleus ^{62}Zn has been studied in a rather detailed way only recently, primarily by the (p,t) reaction at 27.5¹ and 51.9² MeV. Less complete studies of the ($^3\text{He},n$)³ and ($^6\text{Li},d$)⁴ reactions to ^{62}Zn , as well as (p, $2n$)⁵, have yielded additional information about the low-lying states of this neutron-deficient nucleus. The purpose of this study was to determine with good resolution the excitation energies, spins, and parities of levels in ^{62}Zn as seen by the ^{64}Zn (p,t) reaction. As much of the use of the (p,t) reaction as a spectroscopic tool rests upon the extraction of spins and parities by a comparison of the shapes of the angular distributions with those from states of known J^π , the reaction ^{66}Zn (p,t) ^{64}Zn was also studied at the same bombarding energy of 35 MeV. More information is available on ^{64}Zn as it is amenable to inelastic scattering studies. However little information has been gathered on ^{64}Zn via the (p,t) reaction, since earlier studies⁵ were done with poor resolution. Therefore, new information regarding the energy levels in ^{64}Zn could also be obtained in this experiment.

II. EXPERIMENT

The experiment used a beam of 35 MeV protons from the Michigan State University sector-focused cyclotron. The outgoing tritons were bent by an Enge split-pole spectrograph and, when using a thick (1.0 mg/cm²) self-supporting target, were incident upon a single-wire

proportional counter in the spectrometer focal plane. The wire counter was mounted in front of a plastic scintillator which allowed gating of the tritons. A resolution of 35 to 40 keV was obtained by this method. Angular distributions were taken for laboratory angles between 30 and 90°.

A higher resolution study at several angles for both nuclei was also carried out by using a thin (200 $\mu\text{g}/\text{cm}^2$) carbon-backed target and Kodak 25 μ NTB photographic emulsions. The exposed plates were hand-scanned and 20 keV resolution obtained. Typical triton spectrum from these thin-target runs are shown in Fig. 1 for the reaction $^6\text{LiZn}(p,t)^6\text{Zn}$ and in Fig. 2 for $^6\text{LiZn}(p,t)^6\text{Zn}$.

III. RESULTS AND DISCUSSION

A list of the excitation energies determined for ^6Zn is given in Table I and for $^6\text{LiZn}$ is given in Table II. The excitation energies were calibrated at several angles for each nucleus using as reference peaks the 0.0, 0.957, 1.801, and 3.216 MeV levels in ^6Zn and the 0.0, 0.592, 1.800, and 2.609 MeV levels in $^6\text{LiZn}$. The energies listed are generally given to ± 10 keV conservatively, and ± 20 or ± 30 keV at higher excitation energies to allow for uncertainty in extrapolation, as well as for peaks of weaker intensity. The tables also list the spin and parity assignments of this work as well as energy, spin, and parity assignments of other recent work.

A. Distorted-Wave Calculations

Distorted-wave calculations (DWBA) were carried out using the code DWUCK7⁶. The Becchetti-Greenless⁷ proton optical-model parameters were used, and several sets of triton optical-model parameters were tried. These are listed in Table III. It was found that triton sets 1, 2 or 3 all yield angular distributions that are very similar in shape for each angular momenta transfer L considered. Triton sets 4 and 5, which are characterized by a smaller real well depth and which were obtained by extrapolating from the elastic scattering results at 70 MeV, gave poor fits for the $L = 0$ and $L = 2$ angular momenta transfers. Consequently triton set 1, the generalized optical potential for mass 3 projectiles of Becchetti and Greenless, was used for all DWBA calculations shown.

The form factor for $L = 0, 2, 4$ transfers was calculated using simple neutron single particle wave functions of configurations $(r^2 s/2)^2$, $(p^2 s/2)^2$, or a combination of these. The angular-distribution shapes are quite insensitive to the wave functions used, but the magnitudes are not. The wave functions were calculated for a Woods-Saxon potential with $r_0 = 1.25$ fm, $a = 0.65$ fm and a binding energy taken to be one-half the sum of the two neutron separation energy and the excitation energy. A finite-range parameter of 0.69 was used (although no noticeable difference in either magnitude or shape of the angular distributions could be seen when using a value of 0.0) and a range of $\rho = 1.6 \text{ fm}^3$ was employed⁸.

B. ^{64}Zn (p,t) ^{62}Zn

The spins and parities of the states listed in Tables I and II were determined by a comparison with angular distributions of known J^π and with DWBA predictions for a particular L transfer. As seen in some of the following examples, however, the certainty behind some assignments is diminished due to difficulty in distinguishing between $L = 3$ and $L = 4$ transfers and by the marked difference between angular distributions for several known 2^+ states.

Fig. 3 shows angular distributions for a number of states in ^{62}Zn thought to be 0^+ . The ground state angular distribution displays characteristic diffraction-like structure and is fit quite well by the DWBA calculation. The state at 2.33 MeV is peaked at forward angles and shows the same structure as the ground state, so it is most likely the 0^+ member of the two phonon triplet. The integrated cross-section for this 0^+ state is comparable with the 4^+ member of this triplet (2.16 MeV), but is 8 times smaller than the 2^+ member (1.801 MeV). However for ^{64}Zn , where the state at 1.94 MeV is the 0^+ member of the two phonon triplet, the same trend in cross-section ratios is found. The centroid of this triplet in ^{62}Zn is at 2.10 MeV, while it lies at 2.01 and 2.23 in ^{64}Zn and ^{66}Zn respectively; all three nuclei have one phonon 2^+ states at approximately 1 MeV. The 0^+ state at 4.00 MeV in ^{62}Zn is strongly structured and is fit quite well by a $L = 0$ DWBA calculation. The states at 4.62 and 5.24 MeV are probably 0^+ due to their peaking at forward angles.

The 2^+ states are characterized by a secondary maximum at 35° and a forward peaked differential cross-section. Many states fall into this category and are fit fairly well by $L = 2$ DWBA calculations, except that the data are less structured than the theory. Figs. 4 and 5 show angular distributions for several of these states; note the dissimilarity in shapes for the 2^+ states at 0.957 and 1.801 MeV. The state at 3.35 MeV (Fig. 5) is tentatively assigned 1^- due to its observed decreasing cross-section at forward angles.

Angular distributions for 3^- and 4^+ states are shown in Figs. 6 and 7. It is difficult to distinguish between 3^- and 4^+ states in ^{62}Zn in this analysis, which is one of the reasons for studying the ^{66}Zn (p,t) ^{64}Zn reactions, as known 3^- states are populated. The octupole state in ^{62}Zn at 2.74 MeV of Ref. 1 is seen with better resolution to be a doublet of 2.75 (4^+) and 2.81 MeV (2^+). Kusakari et al² assign a possible 3^- to the 2.75 MeV state, yet the decreasing cross-section at forward angles and the similarity to the known 4^+ state at 2.18 MeV make the 4^+ assignment the most probable (see Fig. 6). The strongly populated states at 3.22 MeV and 4.22 MeV are characterized by rather flat angular distributions out to 35° . They are not fit well by either a $L = 3$ or $L = 4$ angular momenta transfer. Comparison with the 3^- state in ^{64}Zn at 3.02 MeV (see Fig. 10) seems to confirm the 3^- assignment given here for these two states, although the shape differences seen between the two 4^+ states in ^{64}Zn at 2.31 and 2.75 MeV tend to make this assignment uncertain. Kusakari² also concludes

that the 3.22 MeV state is 3^- . Recent $^{50}\text{Ni} (0_{1/2}^+, d)$ ^{62}Zn studies⁴ suggest a 3^- state at 3.13 ± 0.02 MeV, although quarter model calculations⁹ predict a 4^+ state at this energy. The 3^- collective states in the other zinc isotopes are located at 2.99 MeV (64), 2.79 MeV (66), 2.76 MeV (68) and 2.85 MeV (70), so a 3^- state at 3.22 MeV in ^{62}Zn is not unlikely. The DWBA calculation for $L = 3$ shown for this state in Fig. 6 used the $(g\ 9/2, f\ 5/2)$ configuration, although the shape remains the same for a $(g\ 9/2, p\ 3/2)$ wave function. The spins and parities given in Tables I and II in parenthesis indicate not enough information is available to be certain of the assignment. The possible 4^+ states at 3.92 and 4.09 might be the 3.87 and 4.04 MeV states seen in $(0_{1/2}^+, d)^4$ and assigned $J^\pi \geq 4^+$.

Transition strengths, N_j , for many transitions are listed in

Table I. The cross-section for the (p, t) reaction is given by¹⁰

$$\frac{d\sigma}{d\Omega} = \frac{N \times 9.72}{(2J_f + 1)} \sigma_{DW}$$

where σ_{DW} is the cross-section calculated by the code DWUCK72, J is the spin of the final state, and the constant 9.72 arises from our choice of 1.0 fm^3 for the range parameter. N is obtained by comparing the data with σ_{DW} at the first maximum. These values are listed in Table I. The transferred neutron configuration is assumed to be $(1f\ 3/2)^2$ for all $L = 0, 2, 4$ transfers, and $(g\ 9/2, f\ 5/2)$ for $L = 3$. Complete wave functions for both the initial and final states are not available, so N is only an arbitrary normalization constant. The use

of a $(2p\ 3/2)^2$ configuration leads to a factor of 6 reduction in the transition strength for the $L = 0, 2$ transfers, and a $(1g\ 9/2, 2p\ 3/2)$ configuration for the 3^- leads to a factor of 25 increase in the transition strength.

C. $^{60}\text{Zn} (p, t)$ ^{64}Zn

Angular distributions for the states observed in ^{64}Zn are shown in Figs. 8-10. Again spin and parity assignments were made by comparison to angular distributions of states of known J^π and to DWBA calculations for a particular L transfer at the appropriate excitation energy. 0^+ states are observed at 0.0, 1.94, 2.61 and 3.24 MeV and are characterized by their sharp structure and forward-peaked angular distributions. Data at $\theta_L = 3^\circ$ is quite helpful here, as seen in Fig. 8. DWBA calculations fit this data quite well, except for a 2° shift relative to the data for the first two 0^+ states. This shift is produced by all of the triton parameter sets listed in Table III. In spite of less complete data, the weakly-excited states at 4.01 and 4.48 MeV were also assigned 0^+ since they are forward peaked. The population of all 0^+ states observed in $^{62}, ^{64}\text{Zn}$ have integrated cross-sections 1-2% of that of the ground state.

Many states were identified as 2^+ because of the observed maximum at 35° and level or slightly peaked cross-sections at the more forward angles. Most of these 2^+ assignments could also be made on the basis of good $L = 2$ DWBA fits, as seen in Fig. 9. The 2^+ states at 0.99

and 1.80 MeV have some dissimilar features, such as more structure in the second 2^+ angular distribution; this feature is similar to that observed in ^{64}Zn (p,t) ^{62}Zn and may be associated with the two phonon character of the 1.80 MeV state².

The state at 3.02 MeV is known from (p,p') ¹¹, $(^6\text{Li,d})$ ⁴, and (α,α') ¹² work to be 3^- . Its angular distribution is characterized by a broad maximum out to about 40° , as seen in Fig. 10, and it is not fit by DWBA calculations very well. These features are unlike the $L = 3$ pattern seen in $\text{Ti}(p,t)$ reactions at 27 MeV¹⁰. Using the 3.02 MeV state as a sample for a 3^- state, the assignment of 3^- was made for the level at 4.41 MeV. The 4.41 MeV state is assigned 3^- in (α,α') ¹² work¹² and is fit well here by an $L = 3$ curve. The 4.23 MeV state could be the 4.14 MeV state seen in (p,p') studies at 26 MeV¹³, where a $L = 3$ transfer was assigned. The 4^+ state at 2.31 MeV has a shape characterized by a broad first maximum out to only 25° . The state at 2.75 MeV has a minimum at 0° , and is typical of higher excited 4^+ states.

Transition strengths, B , for the states in ^{64}Zn are given in Table II and were extracted in the same way as for ^{62}Zn . The strengths are comparable for similar states in the two nuclei. Again too large a cross-section is predicted for the 0^+ excited states in both nuclei.

IV. CONCLUSION

The results of this study have been to establish, in more detail than previous work, level schemes for the nuclei ^{62}Zn and ^{64}Zn as seen via the (p,t) reaction at 35 MeV. Using the argument that the shape of the angular distributions are determined by the angular momentum transfer, spin and parity assignments were made for most states up to an excitation energy of 5.3 MeV by comparing to angular distributions for known states in ^{62}Zn and ^{64}Zn . Several new 0^+ levels were determined, including the 0^+ member of the two phonon triplet in ^{62}Zn at 2.33 MeV. DWBA calculations were performed that fit the data satisfactorily, except in the cases of $L = 3$ and $L = 4$ angular momentum transfer. The slight differences in shapes between $L = 3$ and $L = 4$ transfers, as well as differences in shapes among transitions to 4^+ states themselves, make assignments of J^π difficult. However, several new 3^- assignments for states in ^{62}Zn and ^{64}Zn were made, including the state at 3.22 MeV in ^{62}Zn , in agreement with recent heavy ion work.

REFERENCES

1. I. C. Farnwell, J. J. Kraushaar, and H. W. Baer, Nucl. Phys. A136, 545 (1972).
2. H. Kusakari, T. Suehiro, M. Ishihara, H. Kawakami, H. Yoshikawa, and M. Sakai, J. Phy. Soc. Japan 34, 365 (1973).
3. M. B. Greenfield, C. R. Bingham, E. Newman, and M. J. Saltmarsh, Phys. Rev. 06, 1756 (1972).
4. H. H. Gutbrod and R. G. Markham, Phys. Rev. Lett. 29, 808 (1972) and R. Markham, private communication.
5. G. Sassani, N. M. Hintz, and C. P. Kavaloski, Phys. Rev. 136B, 1006 (1969).
6. P. D. Kunz, University of Colorado (unpublished).
7. F. D. Becchetti and G. W. Greenlees, Phys. Rev. 182, 1190 (1969).
8. E. Rost and P. D. Kunz, Nucl. Phys. A162, 376 (1971).
9. H. Faraazi, A. Jaffrin, N. C. Kermaz, J. C. Faivre, J. Gastebois, B. G. Harvey, J. M. Loiseau, and A. Papineau, Annals of Phys. 60, 905 (1971).
10. H. W. Baer, J. J. Kraushaar, C. E. Moss, N. S. P. King, R. E. L. Green, P. D. Kunz, and E. Rost, Annals of Phys. 76, 437 (1973).
11. Nuclear Data Tables 32, No. 3 (1967).
12. N. Alpert, J. Alster, and E. J. Martens, Phys. Rev. 02, 974 (1970).
13. R. K. Johnson and G. D. Jones, Nucl. Phys. A132, 657 (1968).
14. F. D. Becchetti and G. W. Greenlees in Polarization Phenomena in Nuclear Reactions, ed. by H. H. Barschall and W. Haeblerli (1971), p. 682.
15. E. R. Flynn, D. D. Armstrong, J. G. Berry, and A. G. Blair, Phys. Rev. 182, 1113 (1969).
16. P. P. Urone, L. W. Pat, H. H. Chang, and B. W. Ridley, Nucl. Phys. A163, 229 (1971).
17. R. A. Harrichs and D. L. Shaw, Phys. Rev. 06, 1257 (1972).
18. C. B. Fulmer, private communication.

FIGURE CAPTIONS

- Fig. 1 Spectrum of tritons obtained with a photographic emulsion plate for the reaction ${}^6\text{Li}(\text{p,t}){}^6\text{Li}$ at a laboratory angle of 12° for higher excitation energies. The peak numbers correspond to those listed in Table I.
- Fig. 2 Spectrum of tritons obtained with a photographic emulsion plate for the reaction ${}^6\text{Li}(\text{p,t}){}^6\text{Li}$ at a laboratory angle of 15° for higher excitation energies. The peak numbers correspond to those listed in Table II.
- Fig. 3 Angular distributions for 0^+ states populated in the reaction ${}^6\text{Li}(\text{p,t}){}^6\text{Li}$ at 35 MeV. The lines are DWBA calculations normalized to the data, for $L=0$ transfers.
- Fig. 4 Angular distributions for 2^+ states populated in the reaction ${}^6\text{Li}(\text{p,t}){}^6\text{Li}$. The DWBA calculations shown are for $L=2$ transfers, except where noted.
- Fig. 5 Angular distributions for 2^+ states populated in the reaction ${}^6\text{Li}(\text{p,t}){}^6\text{Li}$. The DWBA calculations shown are for $L=2$ transfers, except where noted.
- Fig. 6 Angular distributions for 3^- or 4^+ states populated in the reaction ${}^6\text{Li}(\text{p,t}){}^6\text{Li}$. The DWBA calculations shown are for $L=4$ transfers, except where noted as being for $L=3$.
- Fig. 7 Angular distributions for 3^- or 4^+ states populated in the reaction ${}^6\text{Li}(\text{p,t}){}^6\text{Li}$. The DWBA calculations shown are for $L=4$ transfers, except where noted as being for $L=3$.

- Fig. 8 Angular distributions for 0^+ states populated in the reaction ${}^{66}\text{Zn}(\text{p,t}){}^{66}\text{Zn}$. DWBA calculations, normalized to the data, are shown for $L=0$ transfers.
- Fig. 9 Angular distributions for 2^+ states populated in the reaction ${}^{66}\text{Zn}(\text{p,t}){}^{66}\text{Zn}$. The DWBA calculations shown are for $L=2$ transfers.
- Fig. 10 Angular distributions for 3^- or 4^+ states populated in the reaction ${}^{66}\text{Zn}(\text{p,t}){}^{66}\text{Zn}$. The DWBA calculations shown are for $L=4$ transfers, except where noted as being for $L=3$.

TABLE I: Levels in ^{62}Zn

Peak No.	Present Work			Ref 1		Ref 2		Ref 4	
	E (MeV)	J^π	σ_{max} ($\mu\text{b/sr}$)	E (MeV)	J^π	E (MeV)	J^π	E (MeV)	J^π
1	0.0	0^+	911	0.0	0^+	0.0	0^+	0.0	0^+
2	0.97	2^+	150	0.97	2^+	0.95	2^+	0.96	2^+
3	1.60	1^+	19	1.60	2^+	1.80	2^+	1.80	2^+
4	2.17	0^+	23	2.17	4^+	2.19	4^+	2.17	4^+
5	2.34	0^+	15	2.34	0^+	2.38	0^+	2.38	0^+
6	2.74	2^+	23	2.74	3^-	2.75	3^-	2.75	3^-
7	2.87	2^+	130	2.87	2^+	2.80	2^+	2.80	2^+
8	3.18	2^+	16	3.18	2^+	3.22	2^+	3.18	2^+
9	3.216	3^-	11	3.216	4^+	3.22	3^-	3.18	3^-
10	3.44	2^+	39	3.44	2^+	3.44	2^+	3.44	2^+
11	3.57	2^+	21	3.57	2^+	3.78	2^+	3.78	2^+
12	3.93	2^+	19	3.93	2^+	3.93	2^+	3.93	2^+
13	4.00	2^+	5.6	4.00	2^+	4.00	2^+	4.00	2^+
14	4.16	2^+	4.4	4.16	2^+	4.16	2^+	4.16	2^+
15	4.32	2^+	13	4.32	2^+	4.32	2^+	4.32	2^+
16	4.32	2^+	14	4.32	2^+	4.32	2^+	4.32	2^+
17	4.57	2^+	6.1	4.57	2^+	4.57	2^+	4.57	2^+
18	4.76	2^+	3.8	4.76	2^+	4.76	2^+	4.76	2^+
19	4.86	2^+	1.5	4.86	2^+	4.86	2^+	4.86	2^+
20	5.05	2^+	11	5.05	2^+	5.05	2^+	5.05	2^+
21	5.05	2^+	4.3	5.05	2^+	5.05	2^+	5.05	2^+
22	5.37	2^+	10	5.37	2^+	5.37	2^+	5.37	2^+
23	5.37	2^+	4.3	5.37	2^+	5.37	2^+	5.37	2^+
24	5.37	2^+	3.9	5.37	2^+	5.37	2^+	5.37	2^+
25	5.37	2^+	5.6	5.37	2^+	5.37	2^+	5.37	2^+
26	5.37	2^+	3.9	5.37	2^+	5.37	2^+	5.37	2^+
27	5.37	2^+	5.6	5.37	2^+	5.37	2^+	5.37	2^+
28	5.37	2^+	3.9	5.37	2^+	5.37	2^+	5.37	2^+
29	5.37	2^+	5.6	5.37	2^+	5.37	2^+	5.37	2^+
30	5.37	2^+	3.9	5.37	2^+	5.37	2^+	5.37	2^+
31	5.37	2^+	5.6	5.37	2^+	5.37	2^+	5.37	2^+
32	5.37	2^+	3.9	5.37	2^+	5.37	2^+	5.37	2^+
33	5.37	2^+	5.6	5.37	2^+	5.37	2^+	5.37	2^+
34	5.37	2^+	3.9	5.37	2^+	5.37	2^+	5.37	2^+
35	5.37	2^+	5.6	5.37	2^+	5.37	2^+	5.37	2^+
36	5.37	2^+	3.9	5.37	2^+	5.37	2^+	5.37	2^+
37	5.37	2^+	5.6	5.37	2^+	5.37	2^+	5.37	2^+
38	5.37	2^+	3.9	5.37	2^+	5.37	2^+	5.37	2^+

TABLE II: Levels in ^{64}Zn

Peak No.	Present Work			Ref 11		Ref 1	
	E (MeV)	J^π	σ_{max} ($\mu\text{b/sr}$)	E (MeV)	J^π	E (MeV)	J^π
1	0.0	0^+	335	0.0	0^+	0.0	0^+
2	0.992	2^+	210	0.992	2^+	0.99	2^+
3	1.600	2^+	20	1.600	2^+	1.61	2^+
4	1.800	0^+	5.0	1.800	0^+	1.81	2^+
5	2.31	4^+	3.0	2.31	4^+	2.32	4^+
6	2.609	4^+	16	2.609	4^+	2.609	4^+
7	2.75	4^+	63	2.75	4^+	2.75	4^+
8	2.81	2^+	120	2.81	2^+	2.81	4^+
9	3.02	3^-	39	3.02	3^-	3.02	3^-
10	3.11	4^+	44	3.11	4^+	3.08	4^+
11	3.24	0^+	11	3.24	0^+	3.07	4^+
12	3.30	2^+	37	3.30	2^+	3.07	4^+
13	3.34	2^+	11	3.34	2^+	3.07	4^+
14	3.50	2^+	37	3.50	2^+	3.07	4^+
15	3.60	2^+	3.4	3.60	2^+	3.07	4^+
16	3.78	2^+	7.3	3.78	2^+	3.07	4^+
17	3.92	2^+	34	3.92	2^+	3.07	4^+
18	3.96	2^+	36	3.96	2^+	3.07	4^+
19	4.01	2^+	5.5	4.01	2^+	3.07	4^+
20	4.12	2^+	22	4.12	2^+	3.07	4^+
21	4.29	2^+	9.1	4.29	2^+	3.07	4^+
22	4.33	2^+	16	4.33	2^+	3.07	4^+
23	4.34	2^+	16	4.34	2^+	3.07	4^+
24	4.38	2^+	16	4.38	2^+	3.07	4^+
25	4.41	2^+	16	4.41	2^+	3.07	4^+
26	4.43	2^+	16	4.43	2^+	3.07	4^+
27	4.58	2^+	16	4.58	2^+	3.07	4^+
28	4.66	2^+	16	4.66	2^+	3.07	4^+
29	4.70	2^+	16	4.70	2^+	3.07	4^+
30	4.75	2^+	16	4.75	2^+	3.07	4^+
31	4.81	2^+	16	4.81	2^+	3.07	4^+
32	4.84	2^+	16	4.84	2^+	3.07	4^+
33	4.93	2^+	16	4.93	2^+	3.07	4^+
34	4.98	2^+	16	4.98	2^+	3.07	4^+
35	5.07	2^+	16	5.07	2^+	3.07	4^+
36	5.16	2^+	16	5.16	2^+	3.07	4^+
37	5.22	2^+	16	5.22	2^+	3.07	4^+
38	5.22	2^+	16	5.22	2^+	3.07	4^+

TABLE III: Optical Model Parameters for Zn(p,t)

Set	V (MeV)	r_0 (fm)	a (fm)	w_{vol} (MeV)	w_{surf} (MeV)	r_1 (fm)	a_1 (fm)	Ref.
Parameters:	44.6	1.17	0.75	5	3.6	1.32	.554	7
Set 1	160.7	1.20	.72	31.5		1.40	.84	14
2	164.7	1.16	.732	21.7		1.498	.817	15
3	175.6	1.14	.737	18.3	1.5	1.553	.780	16
4	114.0	1.14	.842	18.4		1.619	.793	17
5	120.0	1.14	.702		18.6	1.278	.805	18

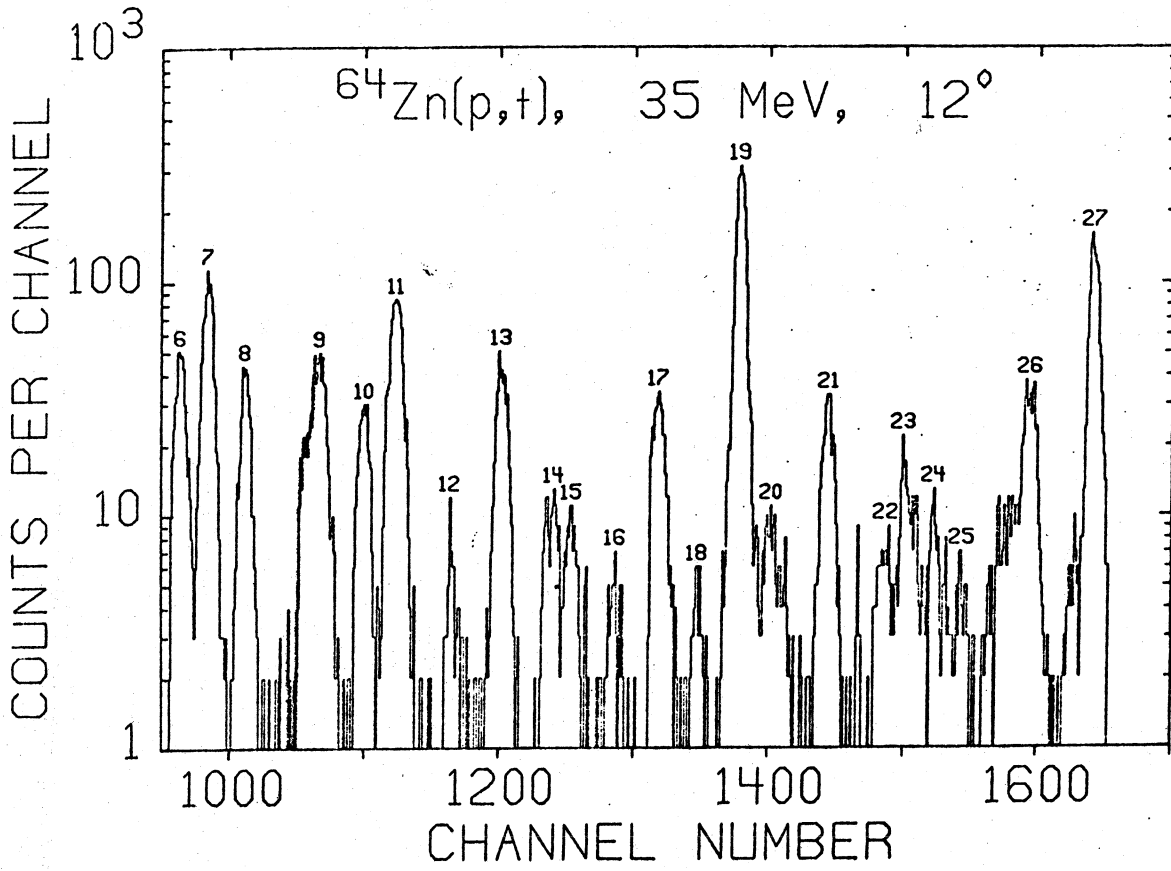


Figure 1

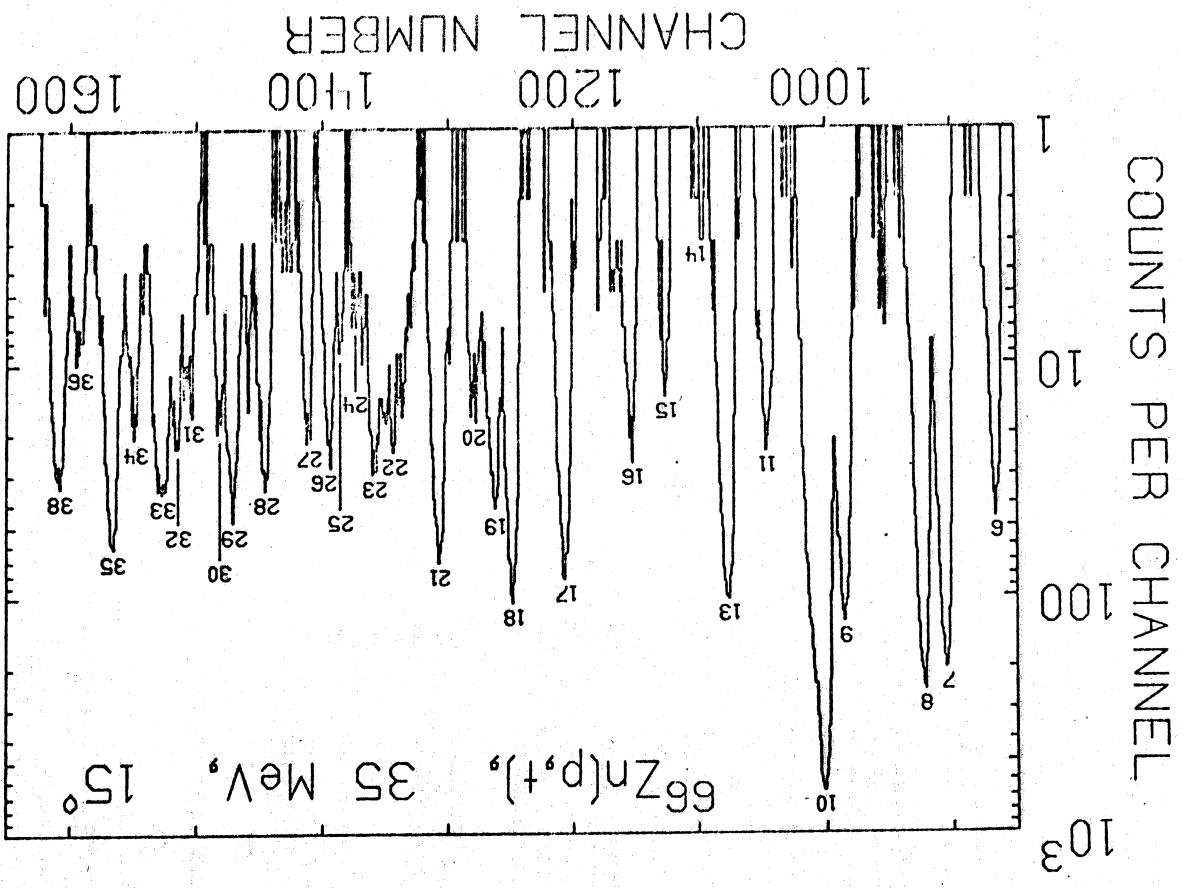


Figure 2

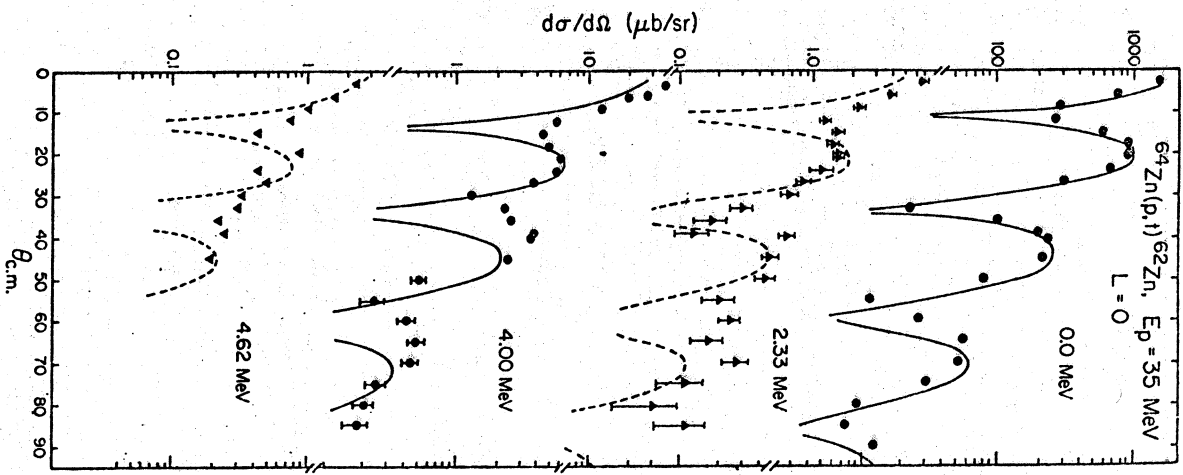


Figure 3

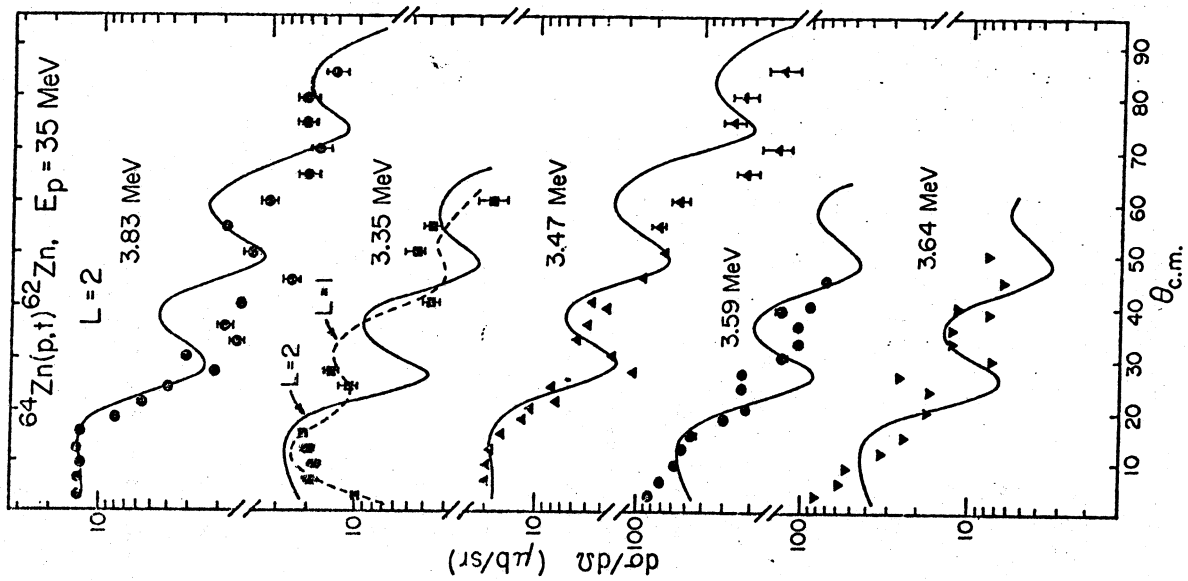


Figure 5

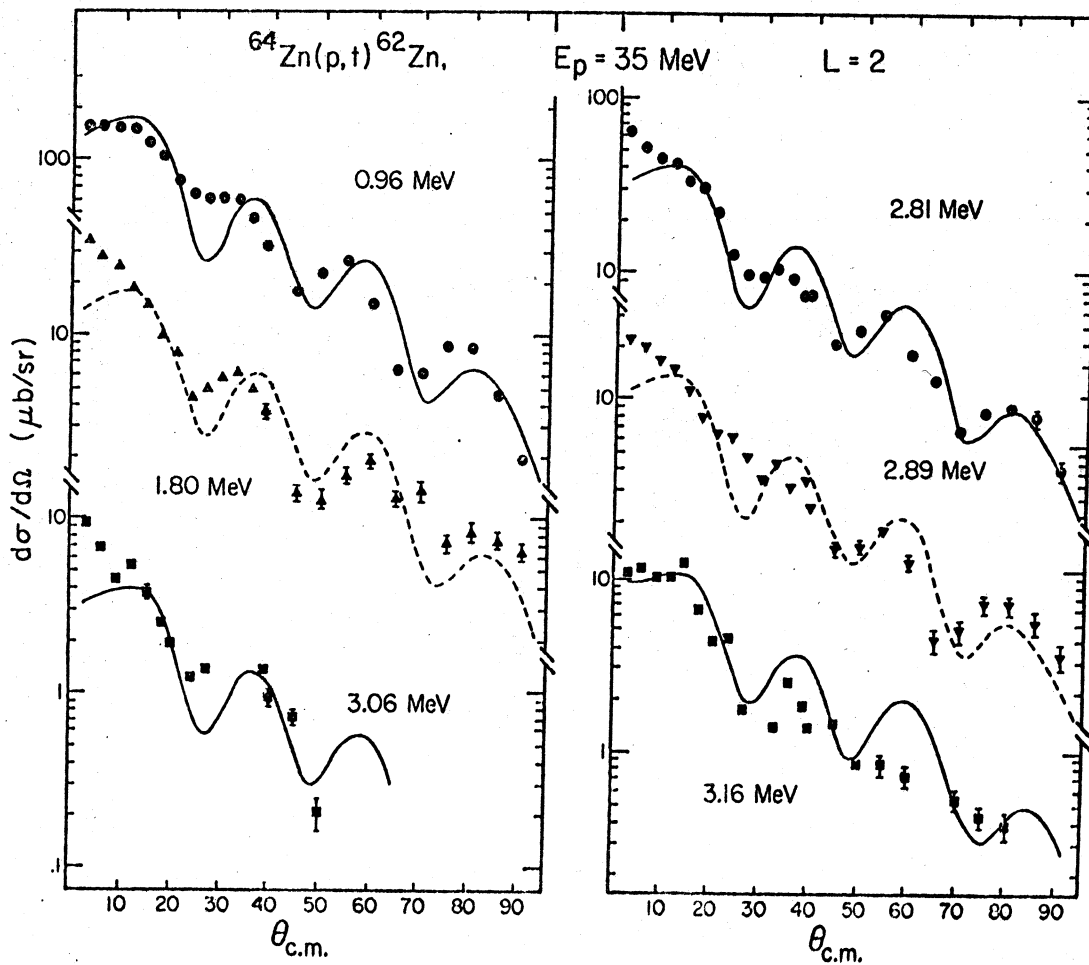


Figure 4

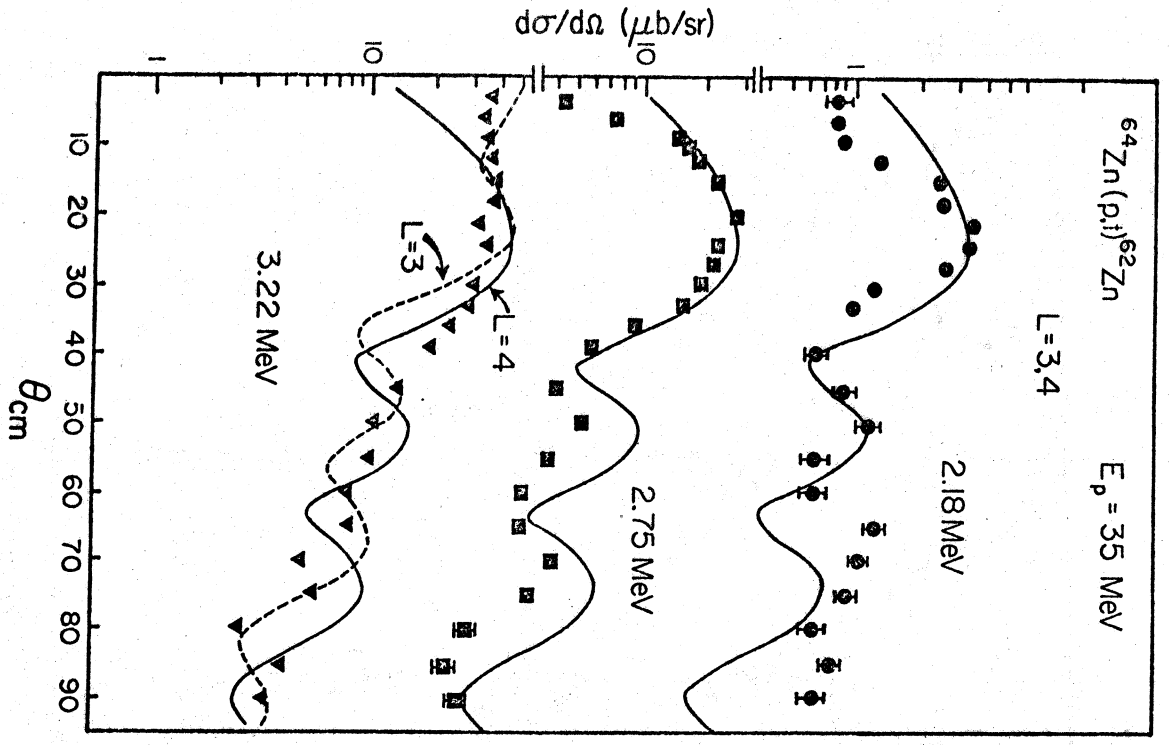


Figure 6

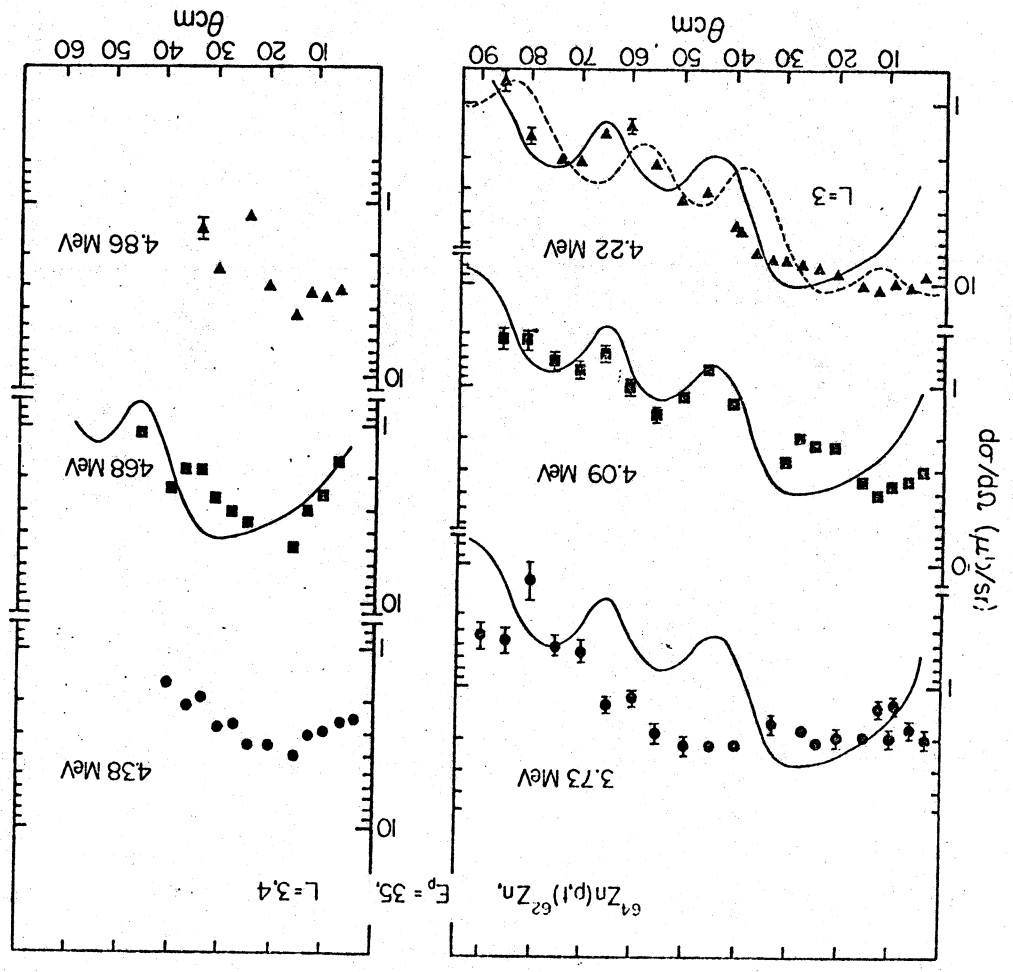


Figure 7

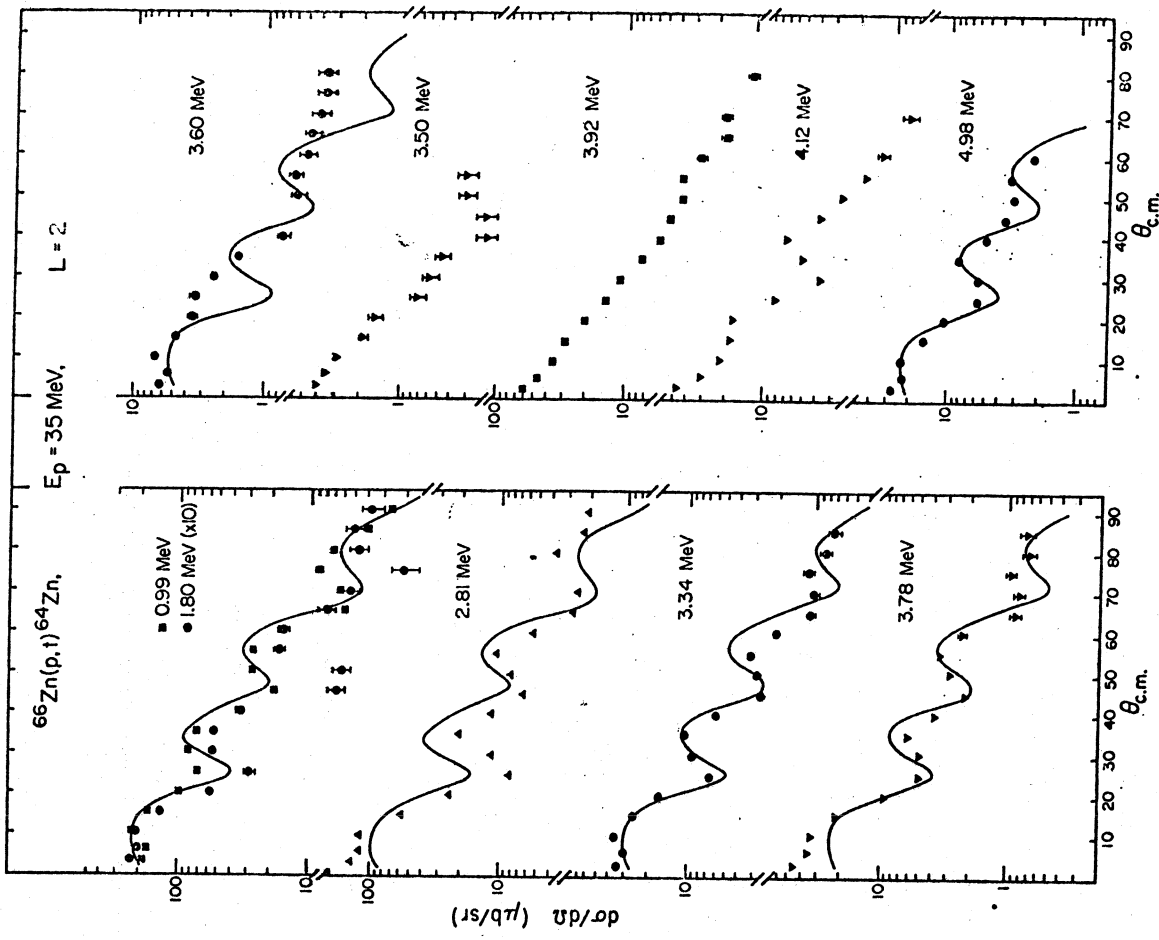


Figure 9

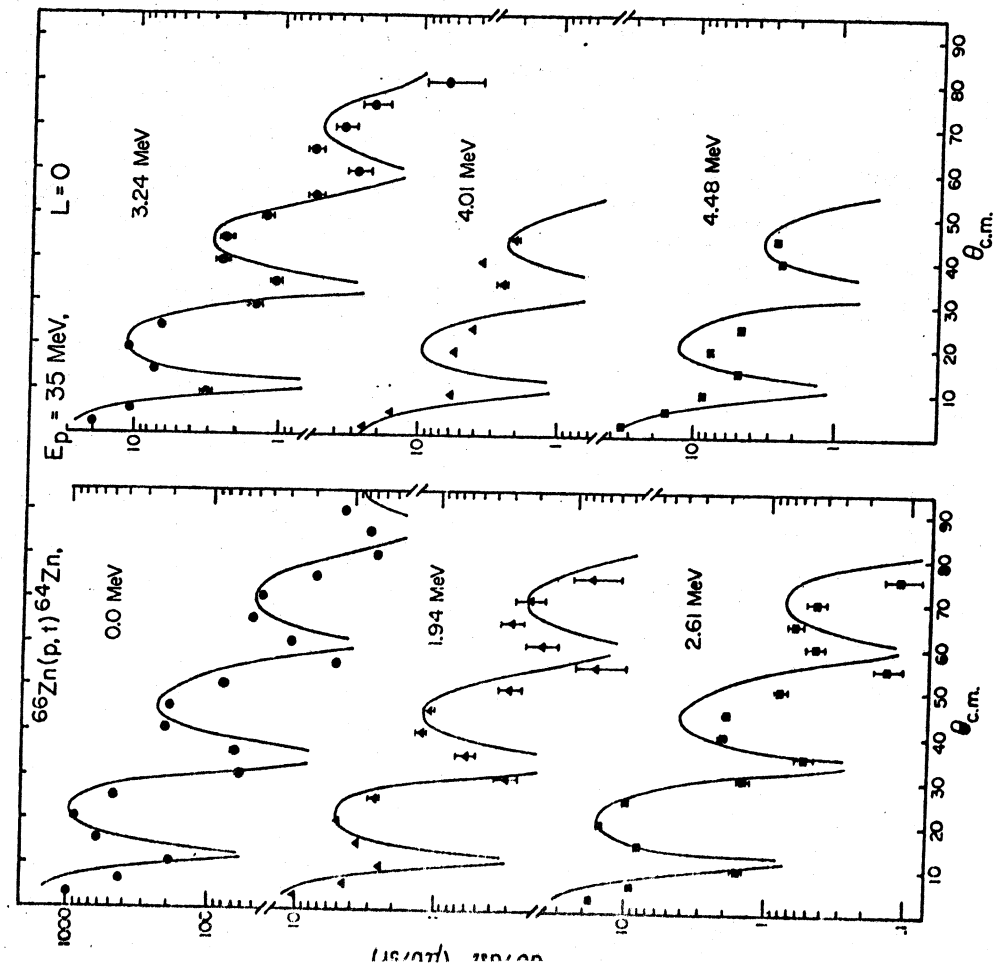


Figure 9

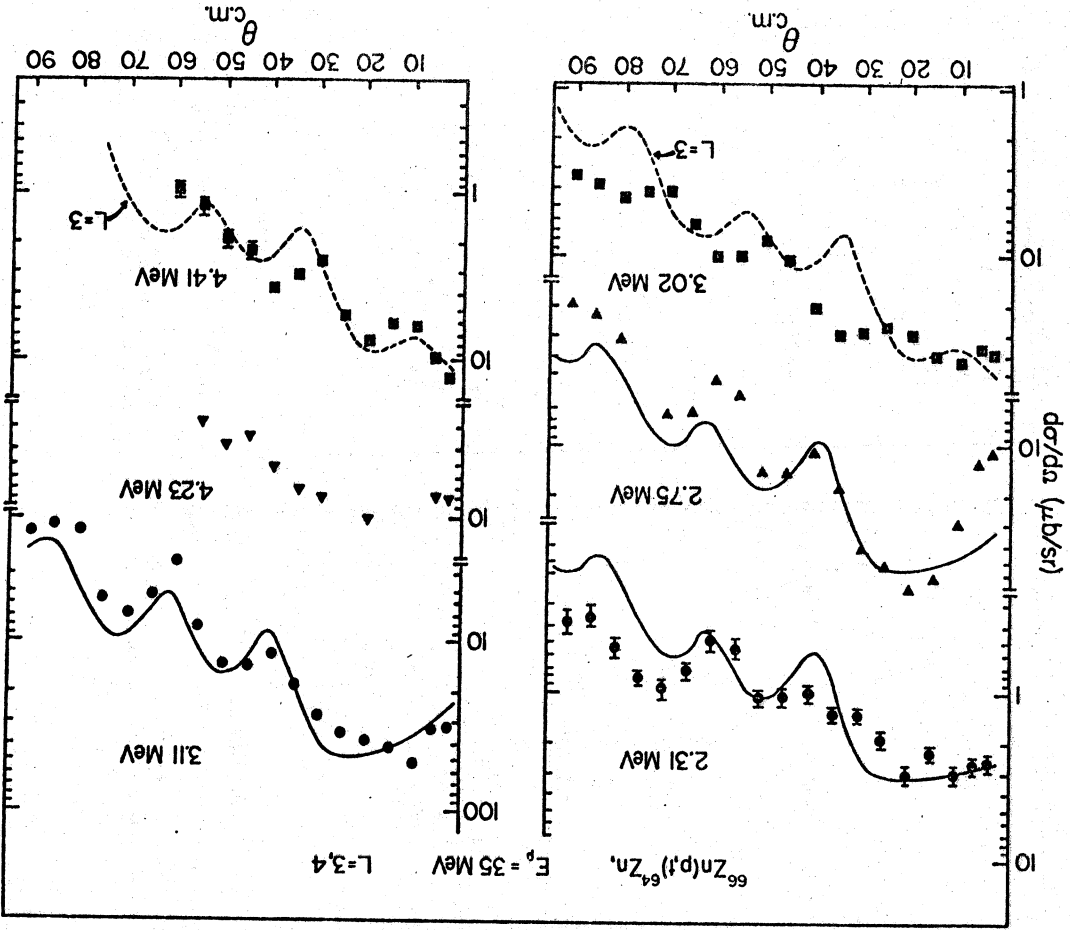


Figure 10